DISCRETE DISLOCATION ANALYSES OF CRACK GROWTH

V.S. Deshpande[1], A. Needleman[1] and E. Van der Giessen[2]
[1]Brown University, Division of Engineering, Providence, RI 02912, USA.
[2]University of Groningen, Dept. of Applied Physics
Nyenborgh 4, 9747 AG Groningen, The Netherlands.

ABSTRACT
Monotonic and cyclic loading of a plane strain mode I crack under small scale yielding are analyzed using discrete dislocation dynamics. The dislocations are all of edge character and are modeled as line singularities in an elastic solid. At each stage of loading, superposition is used to represent the solution in terms of the stress and displacement fields for edge dislocations in a half-space and a non-singular complementary solution that enforces the boundary conditions, which is obtained from a linear elastic, finite element model. The lattice resistance to dislocation motion, dislocation nucleation, interaction with obstacles and annihilation are incorporated into the formulation through a set of constitutive rules. A cohesive surface ahead of the initial crack tip is employed, with either reversible or irreversible relations between the opening traction and the displacement jump in order to simulate cyclic loading in a vacuum and in an oxidizing environment, respectively. It is found that crack growth can occur under cyclic loading conditions above a certain threshold value of ΔK_I; this value is higher in the case of the reversible cohesive law, in line with experimental observations.

KEYWORDS
discrete dislocation plasticity, crack growth, fatigue, environmental effects

INTRODUCTION
The interaction between plastic flow and the actual process of material separation plays an important role in setting the fracture response of structural materials under both monotonic and cyclic loading conditions. In particular, when structural components are subject to high frequency, low amplitude loading, even a typical near-threshold crack growth rate of 10^{-8} mm/cycle prompts designs to be based on the fatigue threshold, $\Delta K_{\rm th}$, of the metal. While threshold values for various metals are well documented, $\Delta K_{\rm th}$ values are known to be sensitive to the microstructure and particularly environmental conditions [1, 2]. Under near-threshold conditions, plastic zone sizes are small and discrete dislocation effects become prominent.

Previous simulations of cyclic crack growth using discrete dislocation models have been carried out, e.g. [3, 4], to gain insight into the mechanisms involved. Such models are specifically geared to cyclic loading, with dislocations nucleated from the crack tip being allowed to glide on specific slip planes around the crack tip. Thus, crack growth in [3, 4] is taken to be deformation controlled in that the crack is assumed to grow by emitting dislocations from the crack tip. In these works, environmental effects are simulated by reducing the stress intensity factor at which a dislocation is emitted from the crack tip.

In this paper, we carry out analyses of crack growth under both monotonic and cyclic loading conditions using the same discrete dislocation framework as in [5, 6]. The fracture properties of the material are embedded in a cohesive surface constitutive relation, and crack initiation and crack growth emerge as natural outcomes of the boundary value problem solution. As emphasis is placed on the environmentally sensitive near-threshold fatigue behavior, both reversible and irreversible cohesive traction-separation relations are employed to investigate cyclic loading in a vacuum and in an oxidizing environment, respectively. The main focus of this study is to ascertain whether the dislocation rearrangement due to cyclic loading can induce crack growth at levels of the applied stress intensity factor lower than needed for crack growth to occur under monotonic loading conditions.

THEORY

The formulation and numerical method follow that in [5, 6] where further details and additional references are given. We consider an infinitely long crack in a two-dimensional single crystal subjected to far field mode I loading, see Fig. 1a. The orientation of the crack is taken to be symmetric to the slip planes in the crystal, so that we need to consider only half of the crystal. Assuming small-scale yielding conditions, a process window

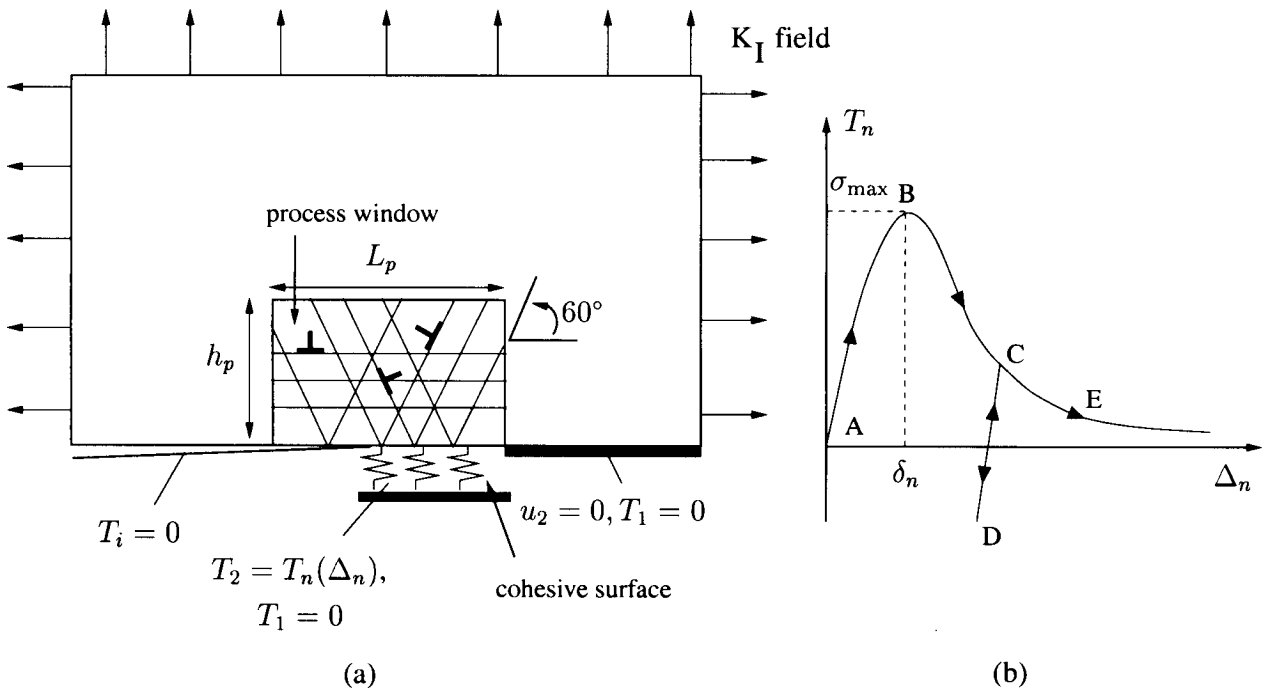

Figure 1: (a) Mode I crack problem with the imposed boundary conditions (b) Irreversible cohesive law.

is centered around the initial crack tip position in which dislocations live on a set of slip systems. The rest of the crystal remains elastic with isotropic properties, specified by the shear modulus $\mu = 26.3$ GPa and Poisson's ratio $\nu = 0.3$. Inside the process window, we assume three slip systems, two with planes at $\pm 60°$ from the crack plane $x_2 = 0$ and one parallel to this plane. The slip plane spacing is $86b$. Only edge dislocations are considered, with Burgers vector $b = 0.25$nm.

Initially, the crystal is assumed to be free of mobile dislocations, but to contain a random distribution of dislocation sources and point obstacles. The sources mimic Frank-Read sources and generate a dislocation dipole when the magnitude of the shear stress exceeds a critical value of $\tau_{\text{nuc}} = 50$MPa during a period of time $t_{\text{nuc}} = 10$ns. The obstacles, which could be small precipitates or forest dislocations, pin dislocations and will release them once the shear stress attains the obstacle strength $\tau_{\text{obs}} = 150$MPa. Annihilation of two dislocations with opposite Burgers vector occurs when they approach each other within a critical annihilation distance $L_{\text{e}} = 6b$. We present calculations for a material with a source and obstacle density $\rho_{\text{src}} = 60/\mu\text{m}^2$ and $\rho_{\text{obs}} = 290/\mu\text{m}^2$, respectively in the process region.

Loading is prescribed in terms of displacements corresponding to the isotropic elastic mode I singular field remote from the crack tip. There is a single cohesive surface [7] that extends over a distance x_c in front of the initial crack (the constitutive equations of the cohesive surface are detailed later in the paper). Ahead of the cohesive surface, symmetry conditions are prescribed. At each time step, an increment of the mode I stress intensity factor $\dot{K}_I \Delta t$ is prescribed. At the current instant, the stress and strain state of the body is known, and the forces on all dislocations can be calculated. On the basis of these forces we update the dislocation structure, which involves the motion of dislocations, the generation of new dislocations, their mutual annihilation, their pinning at obstacles, and their exit into the open crack. After this, the new stress and strain state can be determined. For this purpose, we use superposition [8],

$$u_i = \tilde{u}_i + \hat{u}_i\,, \quad \epsilon_{ij} = \tilde{\epsilon}_{ij} + \hat{\epsilon}_{ij}\,, \quad \sigma_{ij} = \tilde{\sigma}_{ij} + \hat{\sigma}_{ij}\,. \tag{1}$$

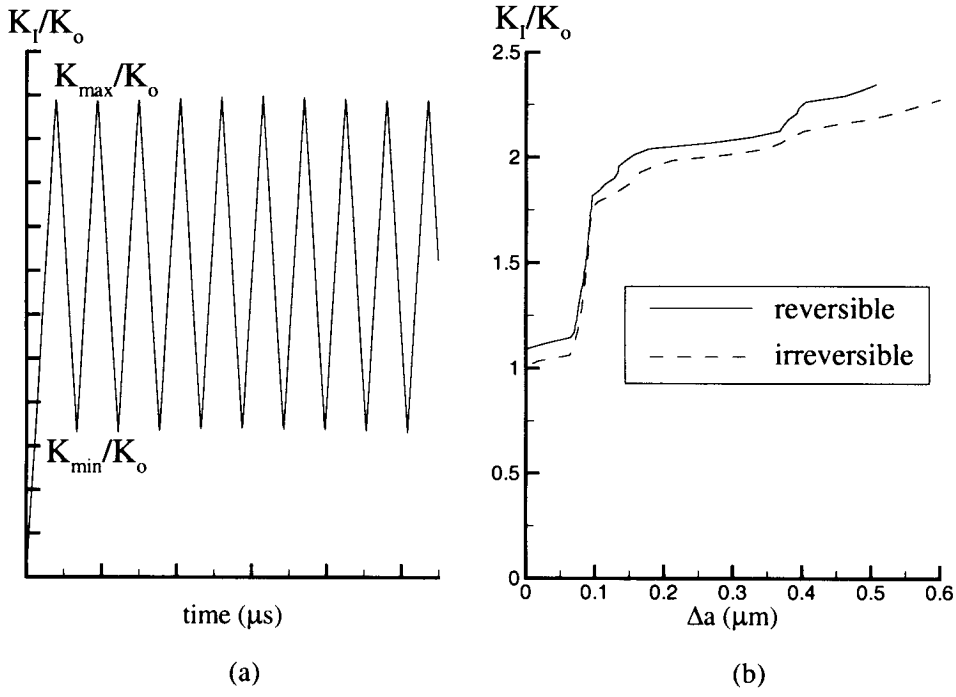

Figure 2: (a) Schematic of the applied stress intensity factor as a function of time (b) Applied stress intensity factor K_I/K_o versus crack extension Δa for monotonic loading with the reversible and irreversible cohesive surface laws.

The $\tilde{(\ )}$ fields are the superposition of the singular fields of the individual dislocations in their current configuration while the $\hat{(\ )}$ fields represent image fields that correct for the actual boundary conditions. For the former we use the fields of an edge dislocation in a half-space [9], with the traction-free surface corresponding to the crack plane $x_2 = 0$.

The sum of the $\tilde{(\ )}$ and the $\hat{(\ )}$ fields in (1) gives the solution that satisfies all boundary conditions. Since the $\hat{(\ )}$ fields are smooth in the region of interest, the boundary value problem for them can conveniently be solved using a finite element method. The size of the region analyzed is 1000μm $\times$ 500μm and a finite element mesh of 120×100 bilinear quadrilateral elements is used. The process window in Fig. 1a is specified by $L_{\rm p} = 10\mu$m and $h_{\rm p} = 12.5\mu$m and is discretized with a fine mesh of 80×80 quadrilateral elements.

With the decomposition (1), the Peach-Koehler force $f^{(k)}$ acting on the kth dislocation is given by

$$f^{(k)} = n_i^{(k)} \left(\hat{\sigma}_{ij} + \sum_{m \neq k} \sigma_{ij}^{(m)} + \Sigma_{ij}^{(k)} \right) b_j^{(k)} . \tag{2}$$

Here, $n_i^{(k)}$ is the slip plane normal, $b_j^{(k)}$ is the Burgers vector and $\Sigma_{ij}^{(k)}$ is the image field on dislocation k due to the traction-free surface, i.e. the difference between the half-space and infinite medium fields. The direction of the Peach-Koehler force is in the slip plane and normal to the dislocation line. The rules for dislocation nucleation and motion are based on this force as the driving force. Dislocation motion is assumed to occur only by glide with no cross slip. The magnitude of the glide velocity $v^{(k)}$ of dislocation k is taken to be linearly related to the Peach-Koehler force $f^{(k)}$ through the drag relation $f^{(k)} = Bv^{(k)}$. The value for B is taken as $B = 10^{-4}$Pa s, which is representative for aluminum [10].

The centerpiece of the present approach is the inclusion of both reversible and irreversible cohesive traction-displacement relations to simulate cyclic loading in non-oxidizing (vacuum) and oxidizing environments, respectively. We start by considering monotonic opening of the crack. The opening is resisted by cohesion at

the atomistic scale and we assume that the normal cohesive traction T_n has the universal binding form [11],

$$T_n(\Delta_n) = e\sigma_{\max}\frac{\Delta_n}{\delta_n}\exp(-\frac{\Delta_n}{\delta_n}), \tag{3}$$

where Δ_n is the total separation of the cohesive surface, $\Delta_n = 2u_2(x_2 = 0)$, and T_n is the traction normal to the cohesive surface. As the cohesive surface separates, the magnitude of the traction increases, reaches a maximum and then approaches zero with increasing separation. In a vacuum, there is no oxidation of the newly formed surface and it is expected that this relation is followed in a reversible manner. However, even in normal atmospheric conditions the newly formed surfaces oxidize and the cohesive law will not follow the above universal binding relation in a reversible manner. We model the effect of the formation of the oxide layer and the subsequent surface contact during unloading by specifying unloading from and reloading towards the monotonic cohesive law to occur according to the incremental relation

$$\dot{T}_n(\Delta_n) = \frac{e\sigma_{\max}}{\delta_n}\dot{\Delta}_n. \tag{4}$$

An example of a typical T_n–Δ_n path for the irreversible cohesive law is shown schematically in Fig. 1b.

The parameters used in this study are $\sigma_{\max} = 0.6\,\text{GPa}$ and $\delta_n = 4b$ giving a work of separation $\phi_n = e\sigma_{\max}\delta_n$ of 1.63 J/m^2. The work of separation can be related to a reference stress intensity factor K_0 defined by

$$K_0 = \sqrt{\frac{E\phi_n}{1-\nu^2}}, \tag{5}$$

where for the material parameters here $K_0 = 0.358\,\text{MPa}\sqrt{\text{m}}$. Note that crack growth in an elastic solid with the given cohesive properties takes place at $K_I/K_0 = 1$. The value of $\sigma_{\max}$ used is about a factor of four smaller than would be appropriate for aluminum. This small value of the strength was used for numerical convenience, since the length scale over which large gradients occur is proportional to $(E/\sigma_{\max})\delta_n$.

RESULTS

In the calculations presented here the applied stress intensity was varied with time between $K_{\min}$ and $K_{\max}$ as shown schematically in Fig. 2a. The calculations were carried out for a loading rate of $\dot{K}_I = 100\text{GPa}\sqrt{\text{m}}/\text{s}$. This rather high loading rate was chosen to reduce the computer time needed for the crack growth calculations because resolving the dislocation dynamics requires a small time step of $\Delta t = 0.5\text{ns}$. For comparison purposes, calculations with K_I monotonically increasing were also carried out. The monotonic crack growth behavior with both the reversible and irreversible cohesive laws are approximately the same. Crack growth initiates at $K_I/K_0 \approx 1.0$. This is followed by substantial plasticity and a sharp rise in the resistance to crack growth (Fig. 2b).

The near-threshold fatigue behavior of metals is known to be sensitive to the stress ratio $R = K_{\min}/K_{\max}$. We present results for $R = 0.3$, but for various values of ΔK_I. First we consider the reversible cohesive surface law. Figure 3a shows the time evolution of crack growth, Δa, under cyclic loading conditions. For both values of ΔK_I, there is an initial "burst" of crack growth. Subsequently, for the case with $\Delta K_I/K_0 = 1.12$ the behavior settles down to an incremental crack growth of the order of $10^{-4}\mu$m/cycle. This corresponds to a crack growth of about one lattice spacing per cycle and is the commonly used operational definition of the threshold crack growth rate [1]. However, for the lower value of $\Delta K_I/K_0 = 0.98$, no cycle-by-cycle crack growth is seen. Further insight into this behavior is gained by examining the evolution of the dislocation density (Fig. 3b). For the case with $\Delta K_I/K_0 = 1.12$ the dislocation density is seen to slowly accumulate with the number of cycles. On the other hand, with $\Delta K_I/K_0 = 0.98$, plastic shakedown takes place resulting in no cycle-by-cycle increase in the dislocation density. Thus, we see that irreversibility of the dislocation motion above a certain threshold value of ΔK_I results in an evolving dislocation structure with cyclic loading; this permits the crack to grow to different lengths during different loading cycles.

Next, we consider cyclic loading with the irreversible cohesive law. Figure 4 shows the time evolution of crack growth with $\Delta K_I/K_0 = 0.77$ and 0.90. We see that incremental crack growth of the order of

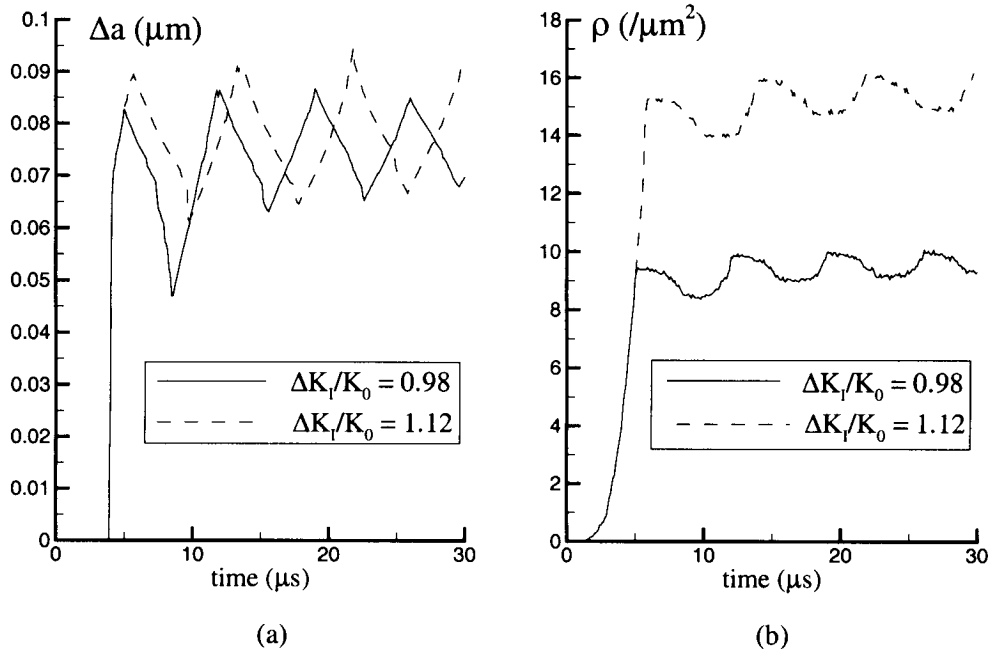

Figure 3: (a) Time evolution of the crack growth and (b) time evolution of the dislocation density for the case with the reversible cohesive surface law ($R = 0.3$).

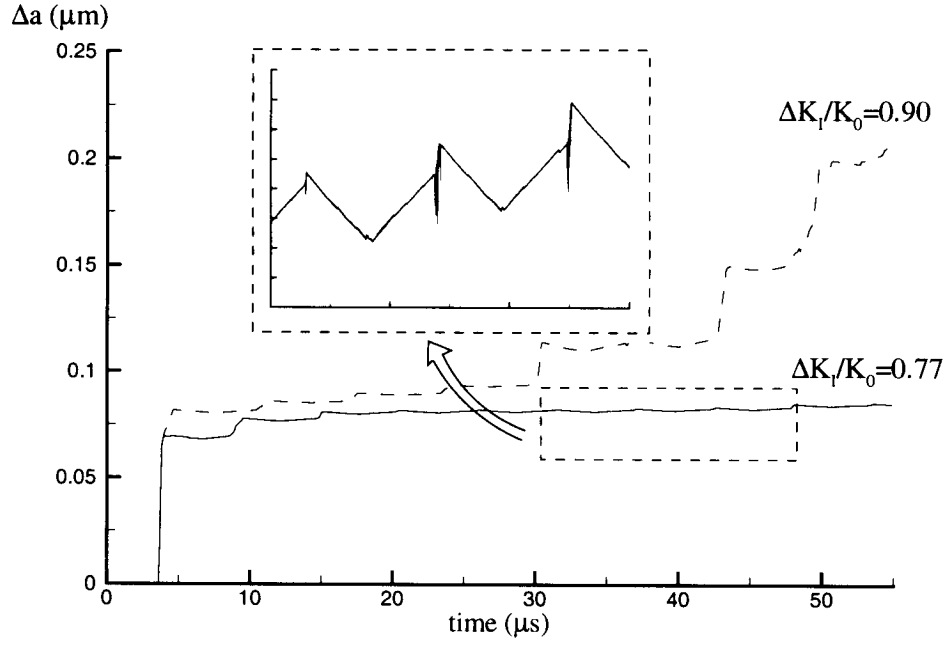

Figure 4: Time evolution of the crack growth with the irreversible cohesive surface law ($R = 0.3$).

$10^{-4}\mu$m/cycle (see inset Fig. 4) occurs in this case at the much lower value of $\Delta K_I/K_0 = 0.77$: a close examination of the inset in Fig. 4 reveals that the incremental crack advance in this case takes place due to a "spurt" of crack growth which occurs towards the end of every loading cycle. It is these "spurts" that result in the incremental cycle-by-cycle crack growth. On the other hand, with $\Delta K_I/K_0 = 0.90$, we are well above the fatigue threshold and crack growth is accelerating. Further calculations are needed to check whether or not

crack growth settles down to a "steady-state" value. It is worth emphasizing that we get continued crack growth under cyclic loading at a value of $K_{\max}$ at which the crack would have arrested under monotonic loading. This is best illustrated by the case with $\Delta K_I/K_0 = 0.90$ ($K_{\max}/K_0 \approx 1.29$ and $K_{\min}/K_0 \approx 0.39$): the crack grows by about 0.2μm after 8 cycles (Fig. 4). However, as seen in Fig. 2b, $K_I/K_0 \approx 2.0$ is needed for the crack to grow by that length under monotonic loading conditions.

CONCLUSIONS

Results of plane strain analyses of mode I crack growth under monotonic and cyclic loading conditions have been presented where plastic flow arises from the motion of large numbers of dislocations. The only difference between the analyses for monotonic and cyclic crack growth is in the specification of the applied loading. The material has three slip systems and is initially dislocation free. Dislocation nucleation occurs from Frank-Read sources distributed randomly in the material, with no special dislocation nucleation from the crack tip. Cyclic loading in a vacuum and in an oxidizing environment are simulated by employing a reversible and an irreversible cohesive law, respectively. Results have been presented for a stress ratio, $R = (K_{\min}/K_{\max}) = 0.3$: the fatigue threshold was calculated by reducing ΔK_I until no cycle-by-cycle crack growth was obtained. Crack growth rates of about $10^{-4}\mu$m/cycle corresponding to typical threshold values were seen with $\Delta K_I/K_0 = 1.12$ and 0.707 for the reversible and irreversible cohesive laws, respectively. Plastic shakedown with no incremental crack growth was observed for ΔK_I lower than these threshold values. In line with experimental observations we found that the fatigue threshold value was higher in a vacuum than in an oxidizing environment.

Fatigue was seen to emerge in the simulations as a consequence of the evolution of internal stresses associated with the irreversibility of the dislocation motion: the dislocation structure and density were different at the beginning and end of each cycle and it was this that permitted cycle-by-cycle crack growth. Moreover, continued crack growth under cyclic loading occurred at a value of $K_{\max}$ for which the crack would have arrested under monotonic loading.

Acknowledgements

Support from the AFOSR MURI at Brown University on *Virtual Testing and Design of Materials: A Multiscale Approach* (AFOSR Grant F49620-99-1-0272) is gratefully acknowledged.

References

[1] Suresh S. (1991). *Fatigue of Materials*, Cambridge University Press, Cambridge UK.

[2] Vasudevan A. K., Sadananda K. and Louat N. (1994). *Mat. Sci. Engin. A* 188, 1-22.

[3] Riemelmoser F. O. and Pippan R. (1997). *Mat. Sci. Engin. A* 234-236, 135-137.

[4] Wilkenson A. J., Roberts S. G. and Hirsch P. B. (1998). *Acta Mat.* 46, 379-390.

[5] Cleveringa H.H.M., Van der Giessen E. and Needleman A. (2000). *J. Mech. Phys. Solids* 48, 1133-1157.

[6] Van der Giessen E., Deshpande V.S., Cleveringa H.H.M. and Needleman A. (2001). *J. Mech. Phys. Solids*, in press.

[7] Needleman A. (1990). *J. Mech. Phys. Solids* 38, 289-324.

[8] Van der Giessen E. and Needleman A. (1995). *Modeling Simul. Mater. Sci. Eng.* **3**, 689-735.

[9] Freund L.B.(1994). *Adv. Appl. Mech.* 30, 1-66.

[10] Kubin L.P., Canova G., Condat M., Devincre B., Pontikis V. and Bréchet Y. (1992). *Solid State Phenomena* 23-24, 455-472.

[11] Rose J.H., Ferrante J. and Smith J.R. (1981). *Phys. Rev. Lett.* 47, 675-678.